AIP | Applied Physics Letters

Temperature dependent transport studies in InN quantum dots grown by droplet epitaxy on silicon nitride/Si substrate

Mahesh Kumar, Basanta Roul, Arjun Shetty, Mohana K. Rajpalke, Thirumaleshwara N. Bhat, A. T. Kalghatgi, and S. B. Krupanidhi

Citation: Applied Physics Letters **99**, 153114 (2011); doi: 10.1063/1.3651762
View online: http://dx.doi.org/10.1063/1.3651762
View Table of Contents: http://scitation.aip.org/content/aip/journal/apl/99/15?ver=pdfcov
Published by the AIP Publishing

Temperature dependent transport studies in InN quantum dots grown by droplet epitaxy on silicon nitride/Si substrate

Mahesh Kumar,[1,2] Basanta Roul,[1,2] Arjun Shetty,[3] Mohana K. Rajpalke,[1] Thirumaleshwara N. Bhat,[1] A. T. Kalghatgi,[2] and S. B. Krupanidhi[1,a)]
[1]*Materials Research Centre, Indian Institute of Science, Bangalore 560012, India*
[2]*Central Research Laboratory, Bharat Electronics, Bangalore 560013, India*
[3]*Department of Electrical Communication Engineering, Indian Institute of Science, Bangalore 560012, India*

(Received 24 July 2011; accepted 25 September 2011; published online 14 October 2011)

InN quantum dots (QDs) were fabricated on silicon nitride/Si (111) substrate by droplet epitaxy. Single-crystalline structure of InN QDs was verified by transmission electron microscopy, and the chemical bonding configurations of InN QDs were examined by x-ray photoelectron spectroscopy. Photoluminescence measurement shows a slight blue shift compared to the bulk InN, arising from size dependent quantum confinement effect. The interdigitated electrode pattern was created and current–voltage (*I–V*) characteristics of InN QDs were studied in a metal–semiconductor–metal configuration in the temperature range of 80–300 K. The *I–V* characteristics of lateral grown InN QDs were explained by using the trap model. © *2011 American Institute of Physics*. [doi:10.1063/1.3651762]

The InN compound has recently attracted much attention, largely due to its narrow direct bandgap energy of ~0.65–0.85 eV.[1,2] This material, if alloyed with other III-nitrides, is very promising for a variety of optoelectronic device applications, such as light-emitting diodes and solar cells, operating from near-infrared to deep-ultraviolet.[3,4] With the rapid progress in epitaxial growth techniques, the nanoscale InN dots with controllable size and density can be grown using molecular beam epitaxy (MBE). InN quantum dots (QDs) are highly interesting owing to nanometer-scale charge carrier confinement in all three spatial dimensions. This gives rise to quantized energies of the QDs leading to applications such as lasers, photo-detectors, light emitting diodes (LEDs), and THz generation. To fabricate InN dots, the Stranski–Krastanow (SK) growth mode and recently the droplet epitaxy (DE) technique has been utilized.[5–8] In DE technique, indium (In) droplets are exposed to a subsequent nitrogen (N) plasma beam to convert the In droplets into InN dots. Compared with other growth techniques, size and density control of the dots are relatively easier in droplet epitaxy, by controlling by the amount of the supplied metals. However, the transport of holes and electrons in QDs is relatively slow. In contrast to bulk semiconductors, charge carriers have to migrate from dot to dot. The position of the energy levels in quantum dots is size dependent. Because of the size distribution in the quantum dot layer, the energy levels are disordered. Charge carrier transport in QDs is, therefore, generally accepted to follow a nonresonant tunneling process.[9,10] In this article, we discuss the fabrication of InN QDs on silicon nitride/Si (111) substrates using an RF plasma nitrogen source, and the results obtained from temperature dependent carrier transport in InN QDs.

The InN QD samples were grown in an radio frequency molecular beam epitaxy (RF-MBE) system. The semi-insulating Si (111) substrates (resistivity > 3000 Ω cm) were chemically cleaned followed by dipping in 5% HF to remove the surface oxide. The substrates were thermally cleaned, and nitrogen plasma was switched on for 1 h at 700 °C substrate temperature, forming a nitridation layer on the surface, while keeping the plasma power and nitrogen flow rate at 350 W and 0.7 sccm, respectively. The substrate was then exposed to an In molecular beam at 100 °C to form In droplets and the exposed time was set to 120 s. The In cell temperature was kept at 830 °C and corresponding beam equivalent pressure (BEP) was 6.7×10^{-7} mbar. Next, the In droplets were exposed for 30 min with nitrogen plasma for nitridation of the In droplets. The nitrogen flow rate and plasma power were 0.7 sccm and 350 W, respectively. In addition, a post-growth annealing at 400 °C was carried out under nitrogen plasma for 30 min. The optical properties were investigated by photoluminescence (PL) measurements using a closed cycle optical cryostat and Ar^+ laser of 514 nm excitation wavelength. Single-crystalline structure of InN QDs is verified by transmission electron microscopy (TEM). The interdigited electrode pattern was created on InN QDs by using photolithography and lift-off techniques. The electrodes were formed by thermal evaporation Al (thickness ~ 150 nm). The distance between the two fingers was 5 μm, and the width of each finger was 5 μm. The length of the finger was ~500 μm. Variable temperature characteristics of the devices were measured using a Keithley-236 source measure unit.

The x-ray photoelectron spectroscopy (XPS) spectrum was acquired using AlK_α radiation ($h\nu = 1486.6$ eV). Figs. 1(a) and 1(b) show the In3d and N1s XPS spectra of InN QDs, respectively. All the binding energies were corrected for the C1s contamination signal (285.0 eV). The In3d core spin-orbit is split to the $3d_{5/2}$ at 444.2 eV and $3d_{3/2}$ peak at 451.7 eV. The peak at around 396.5 eV corresponds to N1s of InN QDs. These results are close to the reported values of InN films.[11] PL spectra were recorded at 10 K and shown in Fig. 1(c), where a strong broad peak was observed at 0.8 eV. Notably, the PL spectrum contained broad peaks and slightly

a)Author to whom correspondence should be addressed. Electronic mail: sbk@mrc.iisc.ernet.in.

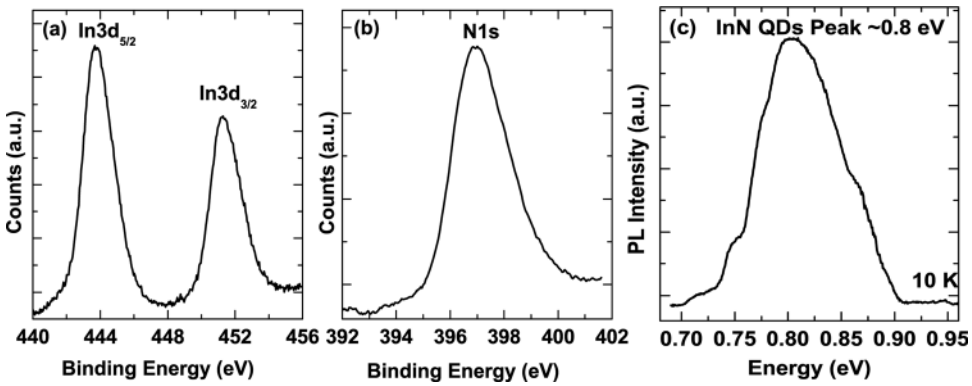

FIG. 1. (a) In3d and (b) N1s XPS spectra of InN QDs. (c) PL spectra of the InN QDs recorded at 10 K and it shows a strong peak emission around ~0.8 eV.

blue shifted compared to the bulk InN, which may be due to the presence of InN QDs with different sizes in the sample and the size dependent quantum confinement effect, respectively. The InN QDs were removed from substrate by sonication in acetone and placed on TEM grids. Figs. 2(a) and 2(b) represent typical transmission electron micrographs and selected area electron diffraction (SAED) of InN QD. The SAED pattern was indexed along the [01-10] zone axis of InN, which represents that InN QDs are single crystalline and the crystal structures of InN dots are hexagonal. The schematic diagram of the device structure is shown in Fig. 2(c). From the diagram it can be seen that InN QDs are isolated from the semi-insulating Si (111) substrate by forming a silicon nitride layer. Figs. 2(d) and 2(e) show the optical microscope images, and Figs. 2(f) and 2(g) show the scanning electron microscopy (SEM) images at different magnifications. From the Fig. 2(f), it can be seen that the InN QDs are uniformly distributed on the substrate. The size of InN QDs is in 20–30 nm range with an overall density of $\sim 5.7 \times 10^{10}\,\mathrm{cm}^{-2}$.

Fig. 3(a) shows the current–voltage (I–V) characteristics of InN QDs at different temperatures in the range 80–300 K. The density of InN QDs is very high, and in between the electrodes there are few paths in which the InN QDs are interconnected. The current flows through these connected InN QDs paths. The I–V characteristics has been analyzed in terms of space charge limited current (SCLC). Because of the size distribution of the InN QDs, the energy levels are disordered. Due to this disorder, the energy distribution of the carrier extended states shrinks and localized states are created. In charge carrier transport, both extended and localized states should play a significant role. The increase in the current with temperature can be attributed to the increase in the carrier density due to excitation of carriers from the localized states to the extended states. This is consistent with the trapping model, which relies on the presence of both the extended states and traps. Hence, the I–V characteristics of lateral InN QDs can be explained by using the trap model,[12,13] considering the exponential distribution of traps in energy and space, as

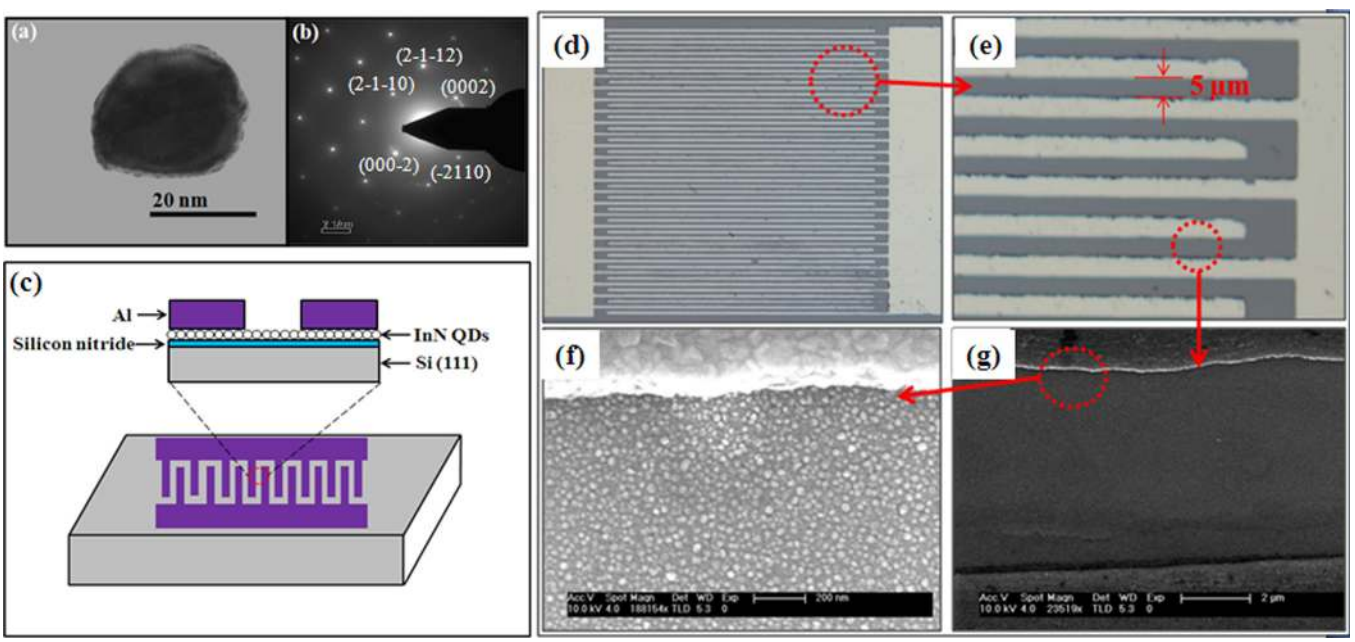

FIG. 2. (Color online) (a) TEM image and (b) selected area electron diffraction (SAED) pattern of InN QD. (c) The schematic diagram of the device structure (not to scale). (d) and (e) The optical microscope images at different magnifications, and (f) and (g) the SEM images at different magnifications. The width and distance between the two fingers is 5 μm and the length of the finger was ~500 μm. From (g), it can be seen that the InN QDs are uniformly distributed between the electrodes.

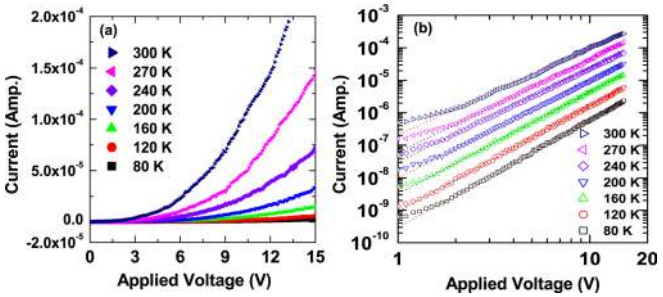

FIG. 3. (Color online) (a) The *I–V* characteristics of device in the temperature range of 80–300 K. (b) The experimental curves and theoretical curves of log–log *I–V* plot of the device are shown by symbols and dotted lines, respectively.

$$N(E) = H_b \exp(-E/E_t), \tag{1}$$

where $N(E) = n(E)E_t$ is the electron trap density at an energy level E below the conduction band edge. Here, $n(E)$ is the distribution function of electron trap density at an energy level E below the conduction band edge (assuming uniform spatial distribution), H_b is the density of traps at the edge of conduction band, and E_t is characteristic trap energy. E_t can also be expressed in terms of the characteristics temperature of trap distribution T_c ($E_t = k_B T_c$), where k_B is the Boltzmann's constant. The trap energy $E = E_t$, Eq. (1) becomes $N(E_t) = H_b/e$, which demonstrates that E_t characterizes the exponential trap distribution and defines the energy level where the trap density has been reduced by $1/e$ of its value at the conduction band edge. Hence, the characteristic width of the exponential distribution is set by the value of E_t.

In case of an exponential distribution of traps (assuming that the trapped electron carrier density (n_t) $\gg$ free electron carrier density (n)) and using the Poisson equation together with the transport equation[14]

$$\frac{dF(x)}{dx} = q[n(x) + n_t(x)]/\varepsilon_s\varepsilon_0, \tag{2}$$

$$J = I/A = q\mu_n n(x)F(x), \tag{3}$$

along with boundary condition

$$V = \int_0^d F(x)dx. \tag{4}$$

If there are no traps, the Poisson equation changes to

$$\frac{dF(x)}{dx} = qn(x)/\varepsilon_s\varepsilon_0, \tag{5}$$

where $F(x)$ is the electric field, d the pitch size of inter-digital capacitor (IDC), $n(x)$ the mobile charge carrier density assumed to be electrons, $n_t(x)$ the trapped electrons density, q the electron charge, ε_s the permittivity of the material, ε_0 is the free-space permittivity, and μ_n is the electron mobility. Area $A = L \times h$, where L is the length of electrode and h is the average height of InN QDs. Assuming $n_t \gg n$ and approximating the Fermi occupancy function by a step function the final solution for *I–V* characteristics for exponentially distributed traps can be written as

$$I = Aq^{1-l}\mu_n N_c \left(\frac{2l+1}{l+1}\right)^{l+1} \left(\frac{l}{l+1}\frac{\varepsilon_s\varepsilon_0}{H_b}\right)^{l} \frac{V^{l+1}}{d^{2l+1}}, \tag{6}$$

where $l = E_t/k_BT = T_c/T$, V is applied voltage and N_c is the effective density of states.

It is seen from Fig. 3(b) that the experimental data at all temperatures from 80 to 300 K show a good agreement to the above mentioned SCLC trap model. Symbols represent the experimental data and dotted lines represent the theoretically generated curves using Eq. (6) at different temperatures. The values of fitting parameters used for this case are: $\varepsilon_s = 15.3$, $\varepsilon_0 = 8.85 \times 10^{-14}$ F/cm, $A = 3.5 \times 10^{-5}$ cm^2, $N_c = 2 \times 10^{20}$ cm^{-3}, $H_b = 5.2 \times 10^{18}$ cm^{-3}, $\mu_n = 300$ cm^2 V^{-1} s^{-1}, and $T_c = 320$ K.

In conclusion, we have fabricated InN QDs on silicon nitride/Si (111) substrate by droplet epitaxy using an RF plasma-assisted MBE system. The size of InN QDs is in the 20–30 nm range, and density of QDs is $\sim 5.7 \times 10^{10}$ cm^{-2}. The TEM analysis shows that InN QDs are single crystalline and the crystal structures of InN dots are hexagonal. The PL spectrum contained broad peaks around $\sim$0.80 eV, which indicated a slight blue shift due to the size dependent quantum confinement effect. The *I–V* characteristics of InN QDs were studied in the temperature range of 80–300 K and were interpreted in terms of space charge limited current using the trap model considering the exponential distribution of traps.

[1]A. A. Klochikhin, V. Y. Davydov, V. V. Emtsev, A. V. Sakharov, V. A. Kapitonov, B. A. Andreev, H. Lu, and W. J. Schaff, Phys. Rev. B **71**, 195207 (2005).
[2]J. Wu, W. Walukiewicz, K. M. Yu, J. W. Ager III, E. E. Haller, H. Lu, W. J. Schaff, Y. Saito, and Y. Nanishi, Appl. Phys. Lett. **80**, 3967 (2002).
[3]A. Yamamoto, M. Tsujino, M. Ohkubo, and A. Hashimoto, Sol. Energy Mater. Sol. Cell **35**, 53 (1994).
[4]H. Lu, W. J. Schaff, J. Hwang, H. Wu, W. Yeo, A. Pharkya, and L. F. Eastman, Appl. Phys. Lett. **77**, 2548 (2000).
[5]C. W. Hu, A. Bell, F. A. Ponce, D. J. Smith, and I. S. T. Tsong, Appl. Phys.Lett. **81**, 3236 (2002).
[6]K. Kawasaki, D. Yamazaki, A. Kinoshita, H. Hirayama, K. Tsutsui, and Y. Aoyagi, Appl. Phys. Lett. **79**, 2243 (2001).
[7]T. Maruyama, H. Otsubo, T. Kondo, Y. Yamamotob, and S. Naritsuka, J. Cryst. Growth **301/302**, 486 (2007).
[8]M. Kumar, B. Roul, T. N. Bhat, M. K. Rajpalke, N. Sinha, A. T. Kalghatgi, and S. B. Krupanidhi, Adv. Sci. Lett. **3**, 379 (2010).
[9]D. Yu, C. J. Wang, B. L. Wehrenberg, and P. Guyot-Sionnest, Phys. Rev. Lett. **92**, 216802 (2004).
[10]A. J. Houtepen, D. Kockmann, and D. Vanmaekelbergh, Nano Lett. **8**, 3516 (2008).
[11]H. Parala, A. Devi, F. Hipler, E. Maile, A. Birkner, H. W. Becker, and R. A. Fischer, J. Cryst. Growth **231**, 68 (2001).
[12]K. Kumari, S. Chand, V. D. Vankar, and V. Kumar, Appl. Phys. Lett. **94**, 213503 (2009).
[13]Z. Chiguvare and V. Dyakonov, Phys. Rev. B **70**, 235207 (2004).
[14]A. K. Kapoor, S. C. Jain, J. Pootmans, V. Kumar, and R. Mertens, J. Appl. Phys. **92**, 3835 (2002).